NUMERICAL INVESTIGATION ON HEAT TRANSFER ENHANCEMENT OF GRAPHENE COATED CIRCULAR PIN FIN

Muhsen Banur ASOUL[1], Kok Hwa YU[1,*], Khaled Ali Mohammad AL-ATTAB[1], Mohd Azmi ISMAIL[1], How Tion PUAY[2]

[1] School of Mechanical Engineering, Engineering Campus, Universiti Sains Malaysia, 14300 Penang, Malaysia

[2] River Engineering and Urban Drainage Research Centre (REDAC), Engineering Campus, Universiti Sains Malaysia, 14300 Penang, Malaysia

[*] Corresponding author; E-mail: yukokhwa@usm.my

The benefit of the graphene coating is twofold. Firstly, the lower temperature on the graphene coated pin fin can be attained, thus ensuring the application system to operate at lower temperatures, preventing overheating. Secondly, the graphene coated fin could yield more uniform distribution of temperature along the pin fin, thereby producing a more uniform heat dissipation along the fin. With such a coating, an improved cooling system can be created, in alleviating the heat transfer limit of conventional heat sink. Numerical results reported in this study revealed that the graphene coating is consistently beneficial for heat dissipation for all cases investigated, regardless of the air velocity, coating thickness, and pin fin length. At the longest pin fin examined, which is 25 D, the temperature difference between the base *and the tip of the pin fin can be reduced to 1.70 K, as compared to 10.60 K temperature difference for the conventional pin fin. Additionally, thermal resistance reduction of up to 56.60 % can be attained using the graphene coating technique.*

Keywords*: CFD, coating, conjugate heat transfer, heat sink, high heat conductivity material*

1. Introduction

The increasing demand for high-performance electronic devices has intensified the demand for more efficient thermal management solutions. Often, heat sinks play a critical role in dissipating heat from electronic components, preventing overheating, and ensuring reliable operation and consistent performance. In recent years, researchers explored the application of highly conductive coatings on heat sink surfaces to enhance the heat dissipation [1-3]. Gan and Hung [1] reported the performance comparison of the graphene nanoplatelet coated sample with the uncoated sample, revealing that the thermal conductance of the 46.9 µm thick coating could exhibit a maximum enhancement of 128 %. The following research works conducted by Balandin *et al.* [2] and Ghosh and Sharma [3] affirming the superiority of graphene material over other materials such as carbon nanotubes and diamond-like carbon coatings, thereby reinforcing the potential of graphene in substituting the conventional materials in high-performance cooling systems. The research works done by Balandin *et al.* [2] demonstrated that the remarkable thermal conductivity of graphene, which exhibit approximately 5300 W/mK, thereby leading to suggestion to adopt this material to improve the heat dissipation in applications including heat sinks, piping systems, and microelectronics. In another study performed by Seol *et al.* [4], the thermal characteristics of graphene has been evaluated. The work highlighted the remarkable improvement of heat transport using suspended graphene, owing to the high thermal conductivity, ranging from 3000 W/mK to 5300 W/mK. Incorporating the graphene material, Yu *et al.* [5] demonstrated the development of the highly thermal conductive epoxy composites, by using dual 3D networks comprised of honeycomb-like porous laser-induced graphene and copper layer.

Apart of the distinctive electrical and optical capabilities of graphene, this material exhibits exceptionally high thermal conductivity. Graphene, owing to its remarkable thermal conductivity, has been thoroughly investigated in improving heat dissipation of heat sinks, in order to effectively cool electronics devices. The technological advancements render graphene as a promising candidate for thermal management applications. As indicated by Wu *et al.* [6], the gains in diversity, morphology, and manufacturing technique shall lead to new innovations, allowing for the extensive application of graphene and substantially evolving the microelectronics business. Amirpour *et al.* [7] demonstrated that the implementation of graphene in the heat sink design. The augmentation made results in a significant heat transfer enhancement, with approximately 24.4 % increase in the heat transfer coefficient. As compared with the aluminium heat sinks, graphene heat sink showed a significant reduction in chip temperature, with reduction of 11.5 %. On the other hand, Cheng *et al.* [8] reported that the carbon nanomaterial-based coating with a water-based epoxy can be applied to provide high dissipating performance. It is demonstrated that the thermal equilibrium temperature of a 15 W LED light bulb can be reduced by 21.3 K. Similarly, Lv et al. [9] showed that graphene yields superior heat transfer performance, demonstrating a 20 – 30 % enhancement in cooling efficacy as compared with the commercially available thermal interface materials (TIMs). In addition, the graphene-based monoliths exhibit superior thermal conductivity in comparison to the graphene/polymer composites, owing to the reduction of high Kapitza resistance at the interface between graphene and the polymer matrix, as a result from the disparity in phonon frequencies at atomically perfect interfaces. According to Hu *et al.* [10], the temperature variation on aluminium and graphene-coated aluminium heat sinks are studied comprising the influence of coating coverage, coating thickness, and heat flux. It is shown that when coating coverage increases from 0 to 100 %, the steady-state temperature decreases by 5 K at the heat flux of 1.8 W/cm. Meanwhile, increasing the average thickness of the graphene covering from 480 nm to 1900 nm would result in a significant temperature reduction of up to 7 K. Furthermore, as the heat flow increases from 1.2 W/cm to2.4 W/cm, the temperature differential between uncoated and graphene-coated samples rises from 1 K to 6 K. The results reported by Hu *et al.* [10] also indicated that, using graphene, the thermal performance improves with the increase in the graphene thickness, but yet bounded to a critical threshold. The study performed by Cheng *et al.* [11] revealed that two essential interfaces (i.e., the contact interface between base and the chip, and the surface of the fins) in the chip cooling system can be simultaneously improved via graphene thermal transport functional material. This augmentation could yield a significant cooling efficiency increase of approximately 30.7 %, indicating that this innovative material holds substantial potential in enhancing the performance of cooling systems. Kung and Yang [12] demonstrated in the study pertaining the natural convective heat transmission, the surface temperature of the graphene-loaded coated aluminium plate can be lowered to 369.85 K, which is 27.4 K lower than that of the bare aluminium plate at 397.25 K, under a heat flow of 16 W. In the scenario involving forced convective heat transfer, the surface temperature diminished from 350.95 K to 341.45 K for a heat flow of 16 W. Fang *et al.* [13] demonstrated a 4.52 K reduction in temperature electronic packaging device using novel composite heat sink structure for a high-power semiconductor laser array with copper-implanted graphite microholes. Praveen *et al.* [14] investigated the performance of the graphene nano-platelets laden micro-encapsulated phase change materials for heat sink application. The performance assessment is made by analyzing the heat sink base temperature over time for specified set point temperatures and the temperature rise rate (TRR). It is reported that the thermal conductivity rose from 0.192 to 0.379 W/mK, and the thermal response rate of the heat sink was postponed arising from the improved heat transport of the novel augmentation. Furthermore, the recovery time of the heat sink reduced owing to diminished thermal resistance and the nucleation effect. Lv *et al.* [15] assessed the new passive heat sink performance, that incorporate the graphene file and polydimethylsiloxane (PDMS) based radiation cooling film. Similar to radiative cooling materials, Graphene/PDMS-TiO2 exhibits a reflectance of 95.5 % in the solar spectrum and merely 2 % in the atmospheric window spectrum. However, the heat conductivity of Graphene/PDMS-TiO2 is an order of magnitude greater than that of conventional, in comparison to the most modern high thermal conductivity, thereby leading to the diminish thermal resistance by 50 %. Dai *et al.* [16] developed graphene thermal interface materials to overcome the high temperature problem of high-power semiconductor devices. The graphene thermal interface materials is reported to have through-plane thermal conductivity up to 176 W/mK and contact thermal resistance as low as 4 – 6 $mm^2 \cdot K/W$.

Apart from enhancing the thermal dissipation of electronics devices, graphene also garners immense interest for its capacity to improve heat dissipation in other applications. Chen *et al.* [17] reported that graphene coating can be utilized to enhance the heat transfer performance of the anti-/deicing component, hence improving its deicing performance. In comparison to the current anti-/deicing methods, maximum efficiency can be enhanced by 70 %. Wang *et al.* [18] findings indicate that the heat accumulated within the phase change composite (PCC) can be dissipated effectively into the environment through two mechanisms: the high thermal conductivity of the graphene PCC and the high thermal emissivity of the graphene layer. With such a design, the battery temperature can be decreased from 344.15 K to 325.65 K utilizing the new design of PCC, without incorporating any active thermal management. Teng *et al.* [19] investigated the use of graphene heat-dissipating coating to promote the cooling performance of automotive light-emitting diode (LED) lamps. The lower temperature attained as compared with the base case, indicates that the graphene coating can serve as a promising coating material for cooling of LED lamps. Pradhan *et al.* [20] employed graphene material to synthesize the aluminium-graphene composite materials for solar thermal collector application.

As thermal management of electronic devices is becoming more important, apart from the heat sink design augmentation (e.g., double layer arrangement [21], augmented fin design [22], etc.), a more viable solution is desired. Among various heat sink configurations, pin fin heat sinks have gained attention due to their enhanced heat dissipation properties through increased surface area and airflow disruption. However, as electronics continue to miniaturize and power densities rise, conventional pin fin heat sinks face limitations in terms of thermal efficiency and size constraints. As postulated by many existing studies, the graphene coating, characterized by their ability to conduct more heat, can significantly enhance cooling efficiency. However, the benefit of the graphene coating on heat sink has not been systematically explored, especially using numerical technique. The lack of insights on the heat transfer enhancement of the graphene coating hampers the potential application of the graphene coating on thermal management applications. This study is thus entailing the implementation of a highly heat conductive graphene coating on an aluminium pin fin. To the best knowledge of the authors, no systematic studies have been conducted on the graphene coated circular pin fin, in particularly on the coating thickness and the geometrical effects of the pin fin. To quantify the extent of heat transfer augmentation induced by the graphene coating, the performance of the augmented pin fin is benchmarked against the conventional pin fin throughout this study.

2. Methodology

2.1. Governing equations

Conjugate heat transfer is employed to assess the heat transfer performance of the graphene coated pin fin. The heat transfer simulation combines both the heat conduction mechanism in solid pin fin and heat convection mechanism in the air domain. The energy equations that govern both the fluid and solid domains are solved simultaneously, together with continuity and momentum equations. The air domain is assumed to have constant thermo-physical properties and it is treated as incompressible Newtonian fluid. The governing equations employed in this study, are stated as follows.

Continuity equation: $$\nabla \cdot \left(\rho_{\mathrm{f}} \vec{V}\right) = 0, \tag{1}$$

Momentum equation: $$\nabla \cdot \left(\rho_{\mathrm{f}} \vec{V}\vec{V}\right) = -\nabla p + \nabla \cdot \left(\mu_{\mathrm{f}} \nabla \vec{V}\right), \tag{2}$$

Energy equations: $$\nabla \cdot \left(\rho_{\mathrm{f}} \vec{V}\, c_{\mathrm{f}}\, T_{\mathrm{f}}\right) = \nabla \cdot \left(k_{\mathrm{f}} \nabla\, T_{\mathrm{f}}\right), \quad \text{(air)} \tag{3}$$

$$\nabla \cdot \left(k_{\mathrm{s}} \nabla\, T_{\mathrm{s}}\right) = 0. \quad \text{(pin fin)} \tag{4}$$

The thermo-physical properties, such as density, dynamic viscosity, specific heat capacity, and thermal conductivity are denoted by ρ, μ, c, and k, respectively. Meanwhile, the velocity, pressure, and temperature fields, are represented by $\vec{V}$, p, and T, respectively. Subscripts f and s are used to indicate the fluid domain and solid pin fin, respectively.

2.2. Geometrical configuration and boundary condition

The present study considers air flow through a single pin fin in a computational domain bounded $(X, Y, Z) \in [0, L_x] \times [0, L_y] \times [0, L_z]$, as shown in Fig. 1. The computational domain length (L_{x}) of 1.5 m, height (L_{y}) of 1.5 m, and width (L_z) of 0.5 m, are employed in this study. The pin fin is of circular shape with diameter of D is positioned at 0.5 m from the upstream of the inlet boundary and at the middle between the left and right boundaries, i.e., 0.25 m from both side boundaries. It is worth to highlight that the influences of the geometrical parameters of the graphene coated pin fin are evaluated based on the pin fin height H and graphene coating thickness t. The geometries of the computational domain employed in this study are stated in Tab. 1.

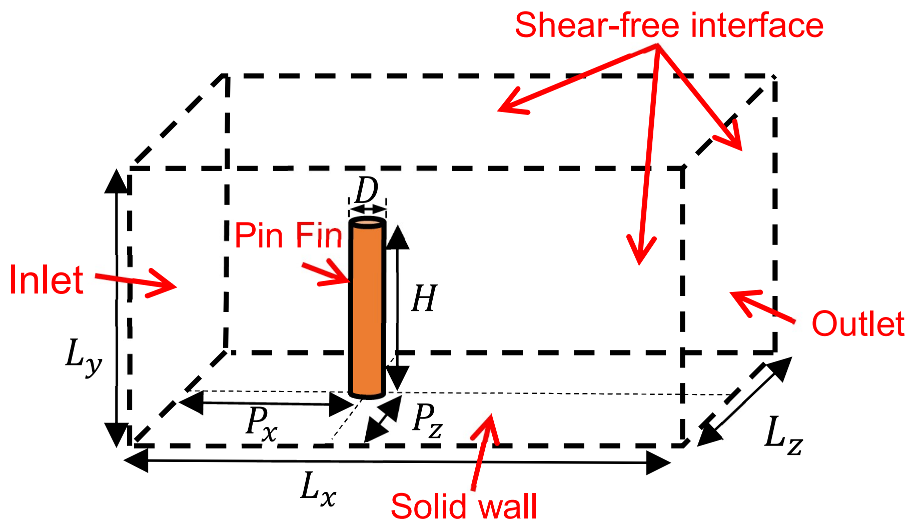

Figure 1. Schematic of flow configuration over heated circular pin fin

Table 1. Flow configuration dimensions

Parameters	Dimensions
Air domain length, L_x [m]	1.5
Air domain height, L_y [m]	1.5
Air domain width, L_z [m]	0.5
Pin fin x-position, P_x [m]	0.5
Pin fin z-position, P_z [m]	0.25

Constant air velocity ranging from 0.1 m/s to 1.0 m/s with a fixed air temperature of 293.15 K is imposed at the inlet. Meanwhile, zero gauge pressure (i.e., 0 Pa) is specified at the outlet. At the bottom of the pin fin, a uniform heat flux (q'') of 5000 W/m^2 is imposed as the heat source. At the top, left, and right boundaries, a shear-free and adiabatic boundary conditions are adopted. The bottom surface is taken to be solid wall with no-slip and adiabatic boundary conditions imposed. On the solid-air interface on the pin fin surface, the system coupling boundary condition is applied. The boundary conditions imposed were summarized in Tab. 2.

Table 2. Boundary conditions imposed on the computational domain

Location	Hydrodynamic BC	Thermal BC
Inlet	Constant inlet velocity	Inlet temperature of 293.15 K
Outlet	Zero gauge pressure	-
Solid wall	No-slip condition	Adiabatic
Shear-free interface	Shear-free condition	Adiabatic
Pin fin bottom surface	No-slip condition	Constant heat flux of 5000 W/m^2
Solid-air interface	No-slip condition	System coupling

The pin fin is made of aluminium and the surface of the pin fin is coated with a layer of graphene. Unless mentioned otherwise, the aluminium pin fin diameter of 0.05 m is employed. The properties of the aluminium and graphene, along with thermo-physical properties of air, are stated in Tab. 3 [23, 24].

Table 3. Thermo-physical properties of air, aluminium, and graphene

Parameters	Air	Aluminium	Graphene
Density, ρ [kg m^{-3}]	1.204	2719	2267
Specific heat capacity, c [J kg^{-1} K^{-1}]	1007	871	700
Heat conductivity, k [W m^{-1} K^{-1}]	0.02514	202.4	3410
Dynamic viscosity, μ [kg m^{-1} s^{-1}]	1.825×10^{-5}	-	-

To quantify the extent of thermal performance enhancement arising from the induction of the graphene coating on the pin fin, the enhancement in thermal performance is evaluated by assessing the reduction of thermal resistance calculated via

$$R = \frac{T_{\max} - T_\infty}{q^{"} A_c}, \tag{5}$$

where the terms of $T_{\max}$, T_∞, $q^{"}$, and A_c denote the maximum temperature of the pin fin, temperature of the air inlet flow, the heat flux applied at the bottom of the pin fin, and the cross-sectional area of the pin fin, respectively. Meanwhile, the flow Reynolds number is defined as follows

$$\mathrm{Re} = \frac{\rho V D}{\mu}, \tag{6}$$

where the terms of $\rho, V,$ and μ refer to density, air inlet velocity, and dynamic viscosity, respectively.

ANSYS Fluent 2024 R1 is employed to solve the governing equations stated in Eqs. (1) – (4). Coupled scheme is used for the pressure-velocity coupling. The spatial discretization of pressure is based on second-order scheme. Meanwhile, second-order upwind scheme is used for the spatial discretization of momentum and energy. The convergence of the solution is attained when the scaled residuals of the continuity, momentum, and energy equations are less than the prescribed value of 10^{-8}.

3. Results and discussion

3.1. Validation of the numerical method

Prior to the numerical data analysis on air flow over graphene coated pin fin, the validity of the numerical simulation was first ascertained. To validate the accuracy of the numerical solution, the temperature profile along the fin height attained using numerical simulation was compared with the exact formulation, given by [25]

$$T(y) = T_\infty + (T_{base} - T_\infty) \exp\left(-y\sqrt{hp/kA_c}\right), \tag{7}$$

where y, p, and A_c are the vertical position, perimeter, and cross-sectional area of the pin fin. The terms k and h refer to the heat conductivity of the air and the convective heat transfer coefficient. Temperature at the bottom of the pin fin is denoted by T_{base}, while the ambient temperature is represented by T_∞. As the exact formulation given in Eq. (7) holds valid for heated long, thin pin fin, a numerical simulation is conducted for validation based on this specific scenario. For the validation case, a $100\ D$ long pin fin with diameter of 0.005 m with the height of 0.5 m is modelled. The ambient temperature of 293.15 K, air flow velocity of 1 m/s, and heat flux of 500 W/m^2 applied at the bottom of the pin fin are employed. As illustrated in Fig. 2, the resulting temperature profile along the vertical axis of the pin fin aligns well with that of the exact formulation. Following the flow and thermal condition of the validation case, the temperature profile calculated from Eq. (7) uses the following parameters: $p = 0.0157$ m, $A_c = 0.0000196$ m^2, $k = 0.2514$ W/mK, $T_b = 293.35$ K, $T_\infty = 293.15$ K, and $h = 0.005$ W/m^{2}K.

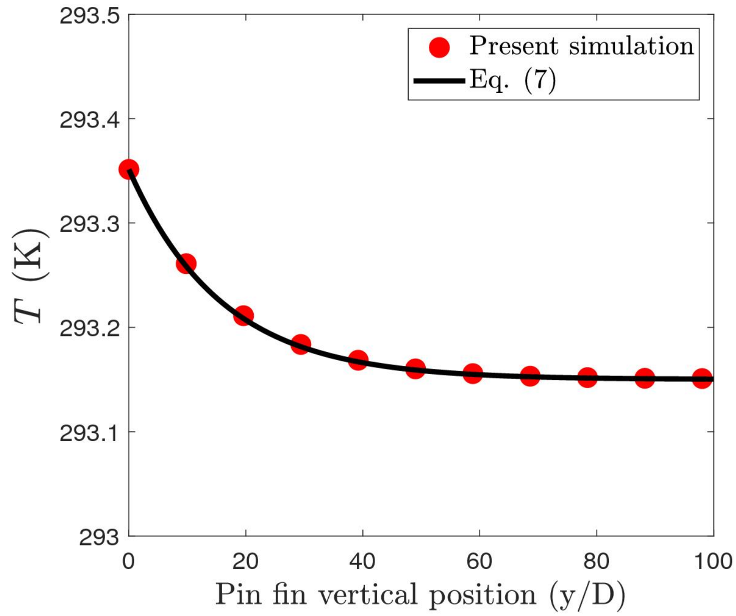

Figure 2. Validation of the temperature profile along the pin fin

3.2. Grid independence test

In this study, mixed structured and unstructured hexahedral grids are employed to mesh both air and solid domains. Finer grid resolution is applied to the air domain in the vicinity of the heated pin fin. The thermal performance based on thermal resistance R of the pin fin are quantified and compared for this grid independence study. Four different grid resolutions (i.e., M1 to M4) with increasing number of elements of 23420, 53395, 187030, and 305384, are employed. For grid independence test, pin fin with diameter of 0.05 m and height of 0.25 m is employed. Constant air inlet velocity of 0.1 m/s and uniform heat flux of 5000 W/m^2 is applied at the bottom surface of the pin fin. The mesh convergence test evaluated is based on the relative error metric of the thermal resistance, given by

$$e_R = \left| \frac{R_{M_x} - R_{M_4}}{R_{M_4}} \right| \times 100\% \, , \tag{8}$$

in which e represents the relative error in comparison to that of the finest grid resolution (i.e., M4). As tabulated in Tab. 4, the relative error of thermal resistance reduces with the increase of the mesh elements

Table 4. Relative error in thermal resistance with respect to the finest grid

Grid	Number of elements	Thermal resistance R [KW^{-1}]	Relative error e_R (%)
M1	23420	6.2338	24.64
M2	53395	5.6450	12.87
M3	187030	5.0064	0.10
M4	305384	5.0013	Baseline

used. As compared with that of grid M4, the deviation on the thermal resistance for grid M3 is only 0.10 %, thereby adopting the M3 grid resolution as the ideal grid resolution for this numerical study.

3.3. Effect of graphene coating thickness

The impact of varying graphene thickness, specifically $t = 0.01\ D, 0.05\ D,$ and $0.1\ D$, on the thermal performance is examined. Employing a constant pin fin diameter of 0.05 m with height of 0.25 m, the employed graphene coating thicknesses correspond to 0.0005 m, 0.0025 m, and 0.005 m, respectively. The pin fin is subjected to a constant heat flux of 5000 W/m^2 applied at its base. To cool the pin fin, air at ambient temperature of 293.15 K is forced over it at 0.1 m/s. As shown in Fig. 3, the temperature of the pin fin reduces with the increase of the graphene coating thickness. Without the graphene coating, aluminium pin fin attains a temperature of approximately 341 K. When the same aluminium pin fin is coated with 0.1 D thick graphene, the temperature drops to around 334 K. This is consistent with the observation reported by Hu et al. [10] that reduction in the temperature is attained when the coating thickness is increased.

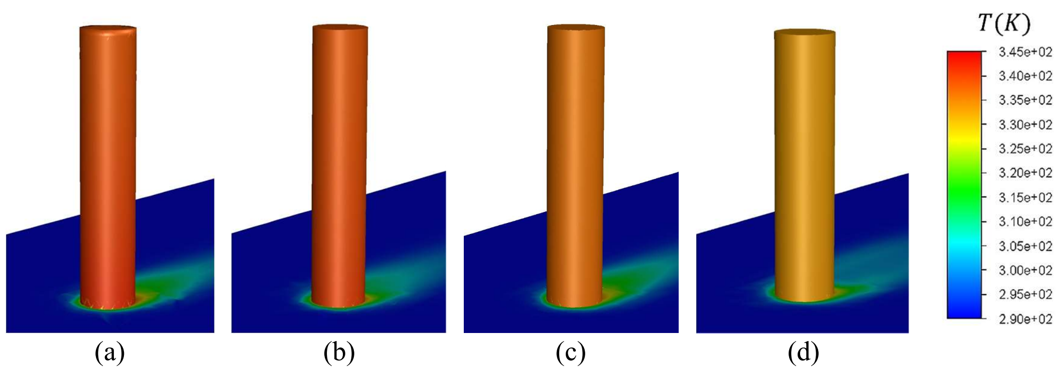

Figure 3. Temperature field on (a) aluminium rod, aluminium rod with (b) $0.01\ D$, (c) $0.05\ D$, and (d) $0.1\ D$ thick graphene coating

The effect of the graphene coating on the pin fin is analyzed to understand the temperature distribution along its length. The resulting temperature profile in the vertical direction is presented in Fig. 4. For the aluminium pin fin, the temperature ranges from 339.07 K to 342.30 K with the highest temperature at the base and the lowest at the tip. As expected, the addition of a graphene coating leads to a steady decline in temperature as the graphene thickness increases. At the pin fin base, the maximum temperature decreases to 340.90 K, 337.57 K, and 334.08 K, for graphene thickness of $0.01\ D, 0.05\ D,$ and $0.1\ D$, respectively. This implies that a maximum temperature reduction of 1.40 K, 4.73 K, and 8.22 K can be achieved with these thicknesses. It suggests that even with a relatively thin graphene layer, such as one-tenth of the pin fin diameter, the overall temperature can be significantly lower. Moreover, thicker graphene coatings lead to smaller temperature variations along the pin fin. For example, with a $0.1\ D$ thick graphene layer, the temperature difference is only 0.36 K, whereas a conventional pin fin would have a 3.23 K difference under the same heating conditions. A more uniform temperature distribution indicates more efficient heat transfer from the fin to the surrounding air, ensuring more evenly heat dissipation along the pin fin, reducing the risk of localized overheating, and improving overall cooling performance.

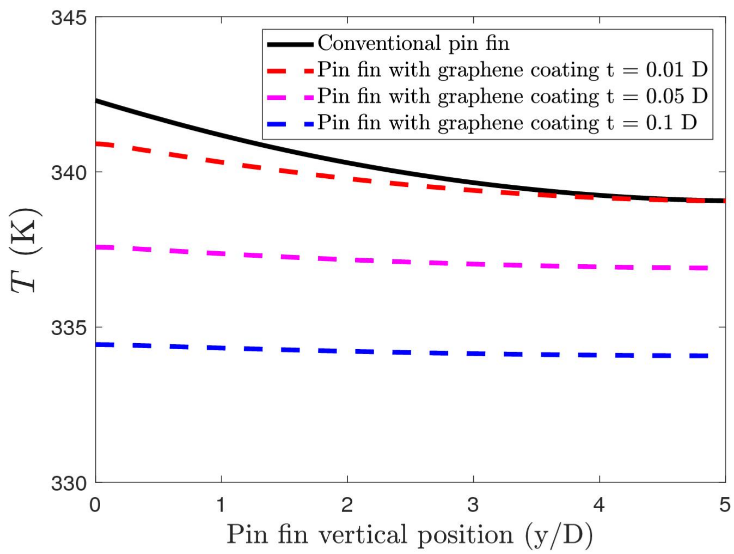

Figure 4. Temperature profile along the pin fin for conventional and graphene coated pin fin

The temperature performance of the graphene coated pin fin is also assessed under different air velocities, ranging from 0.1 m/s to 1.0 m/s, corresponding to Reynolds number of 330 to 3300, respectively. The temperature at the pin fin base is assessed, as the local maximum temperature located at the bottom of the pin fin is of interest. As depicted in Fig. 5(a), a general trend of reducing maximum temperature at the pin fin base is observed for all cases investigated. At air velocity of 0.1 m/s, highest base temperature of 342.30 K is recorded for conventional pin fin. The increase in the air velocity leads to the reduction of the base temperature. The base temperature of the conventional pin fin is 319.88 K when air velocity is forced at 1.0 m/s. As illustrated in Fig. 5(a), the decay rate of the base temperature is observed to be smaller at higher air velocities. With graphene coating, the same base temperature trend is emulated at lower temperature. At air velocity of 1.0 m/s, employing graphene thickness of $0.01\,D, 0.05\,D,$ and $0.1\,D$, the base temperature reduced to 318.46 K, 316.12 K, and 313.84 K. As thermal resistance is proportional to the maximum temperature, the resulting thermal resistance exhibits similar trend, as shown in Fig. 5(b). Lower thermal resistance R attained at higher air velocity, indicating a more efficient heat transfer of the pin fin. With graphene coating, regardless of coating thickness, the thermal resistance is consistently lower. As the graphene coating is thicker, it exhibits lower thermal resistance, consistent in all the air velocities examined. The reduction of the thermal resistance is measured in terms of $\Delta R/R_{\text{CON}}$, with thermal resistance of the conventional pin fin is indicated by R_{CON}. Comparatively, pin fin with thicker graphene coating would yield greater thermal resistance reduction. As depicted in Fig. 6, the $\Delta R/R_{\text{CON}}$ increases fairly with the increase of air velocity. The increase rate of the $\Delta R/R_{\text{CON}}$ is, however, reduced at higher velocities, implicating the vanishing effects of the air velocity on the thermal resistance reduction. At the highest air velocity of 1.0 m/s, the reduction of thermal resistance, arising from graphene coating, is estimated to be 5.3 %, 14.1 %, and 22.6 %, for the case of $0.01\,D, 0.05\,D,$ and $0.1\,D$ thick graphene coating, respectively.

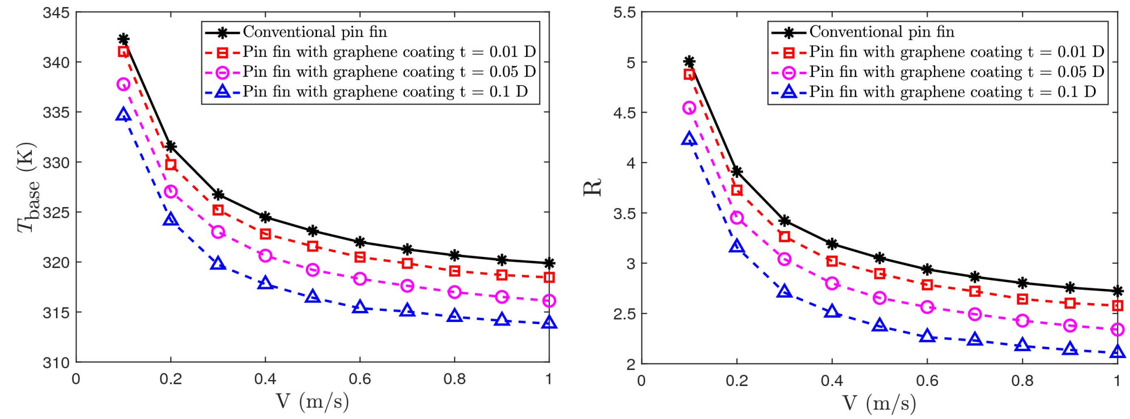

(a) (b)

Figure 5. Variation of (a) maximum temperature and (b) thermal resistance, with respect to the air velocity

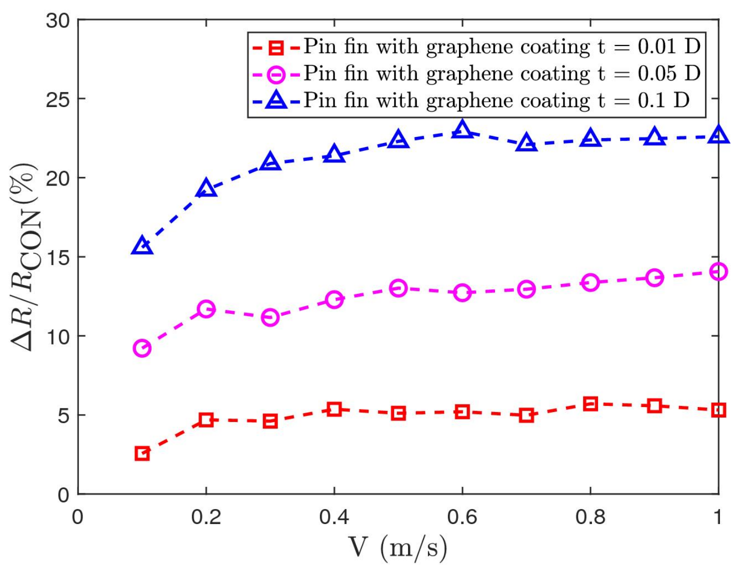

Figure 6. Variation of $\Delta R/R_{\mathrm{CON}}$ with respect to air velocities for graphene coated pin fin

3.4. Effect of pin fin length

The influence of the pin fin length on the thermal performance is also assessed. The thermal performance of the graphene coated pin fin is compared with its conventional counterpart for pin fin length ranging between 1 D to 25 D. The base temperature and the thermal resistance results for air cooling forced at velocity 1.0 m/s are illustrated in Fig. 7. At pin fin length of 1 D, the base temperature are 393.83 K, 393.47 K, and 378.02 K, for conventional pin fin, pin fin with 0.01 D, and 0.1 D thick graphene coating, respectively. This leads to thermal resistance of 10.26, 10.22, and 8.64, respectively. Based on the base temperature and thermal resistance results, it can be inferred that pin fins shorter than 5 D have poor heat transfer efficiency, as evidenced by their higher temperature, even though the same amount of heat is supplied to them. As the length of the pin fin increases, the surface area expands, leading to improved heat dissipation. At 25 D, the base temperature of 305.87 K, 303.21 K, and 298.67 K are attained for the three cases examined. In terms of the thermal resistance, numerical simulations performed predicts that the R to be 1.30, 1.02, and 0.56, for these three cases. In the presence of the graphene coating, significant reduction of the thermal resistance is predicted, as presented in Fig. 8. Regardless of the pin fin height, graphene coating promotes better heat dissipation of the pin fin. Higher thermal resistance can be achieved for longer pin fin. At 25 D long pin fin, graphene coating with thickness 0.01 D and 0.1 D could yield 20.91 % and 56.60 % reduction in thermal resistance.

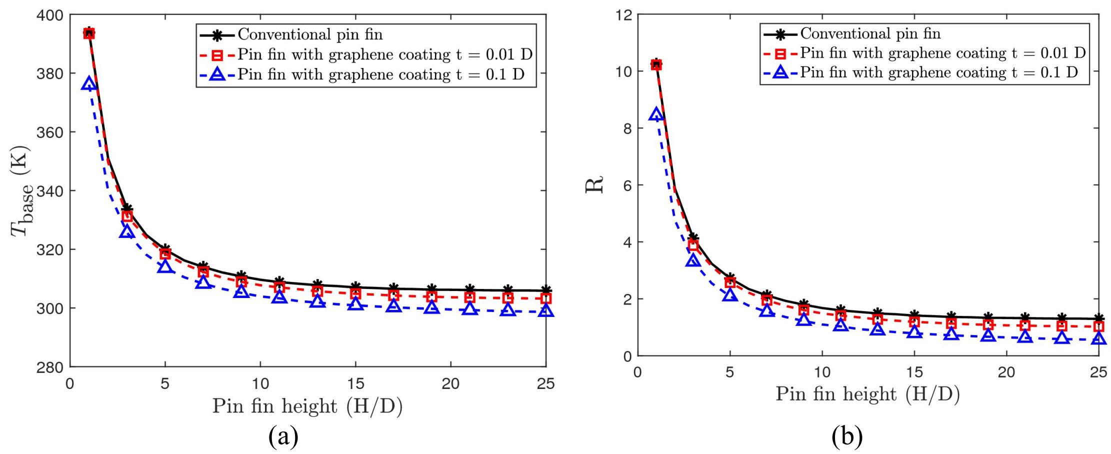

Figure 7. Variation of (a) maximum temperature and (b) thermal resistance, with respect to the pin fin height

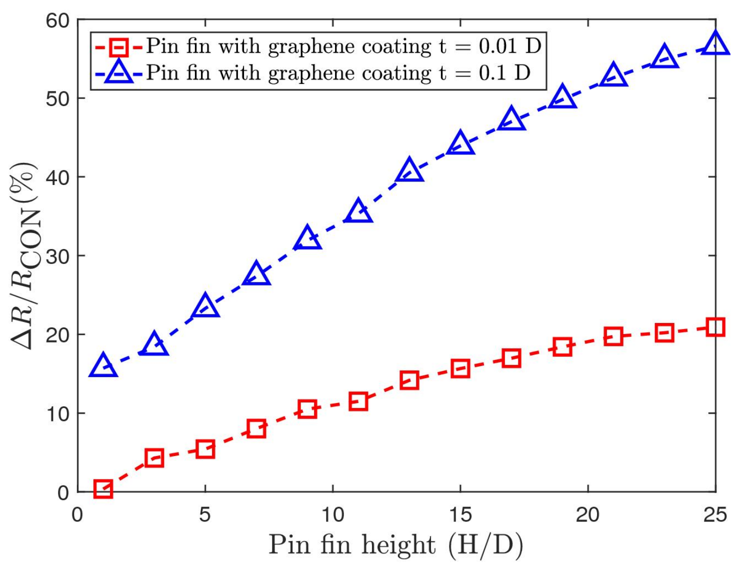

Figure 8. Variation of $\Delta R/R_{\mathrm{CON}}$ with respect to pin fin height for graphene coated pin fin

For pin fin length of 25 D, the temperature profiles along the pin fin length for different cases are plotted in Fig. 9. For the conventional pin fin, the temperature profile ranges from 305.86 K at the base of the pin fin, while the temperature reduces to 295.26 K at the tip. With graphene coating, the maximum temperature at the base reduced to 303.08 K and 298.47 K for the graphene coating thickness of 0.01 D and 0.1 D, respectively. Meanwhile, at the tip, the presence of graphene coating, the temperature is elevated to 295.99 K and 296.77 K for these two cases. These lead to the smaller temperature difference between the base and tip of the pin fin, from 10.60 K for the conventional pin fin, to 7.08 K and 1.70 K for graphene coating thickness of $0.01\ D$ and $0.1\ D$, respectively. In accordance with the attained temperature profile along the pin fin, the graphene coating on the pin fin surface fundamentally elevate the heat conducted along the pin fin from the base to the tip. With graphene layer, heat is not solely conducted through the aluminium substrate but also along the graphene substrate. As indicated by this study, thicker graphene coating significantly enhance the heat conduction through the pin fin, allowing heat to reach the tip more conveniently. For the case of $0.1\ D$, the temperature difference between the wall and the ambient temperature is roughly 3.5 to 5.2 K, yielding more uniform heat dissipation along the pin fin to the surrounding air. For conventional pin fin, the corresponding temperature differences are 12.71 K at the base and 2.1 K at the tip. This leads to uneven heat dissipation with high heat dissipation at the lower portion of the pin fin and low heat dissipation at the upper portion, thereby often give rise to insignificant contribution of the upper portion of the pin fin.

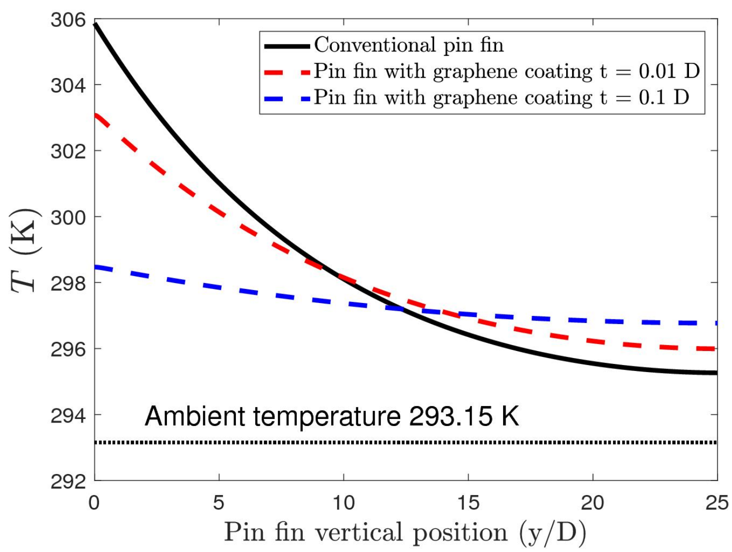

Figure 9. Temperature profile along the pin fin for conventional pin fin and graphene coated pin fin

Similar to other types of fins, the length of a pin fin is often restricted due to reduced heat transfer efficiency in the upper region. Since the additional length contributes little to heat dissipation, the extra weight and material offer minimal benefit. As a result, fins are typically shorter in thermal dissipation applications. However, the numerical results of this study suggest that graphene coating can enhance the effectiveness of longer fins in heat transfer applications. The coating not only promotes more uniform heat transfer along the fin but also lowers the maximum temperature, helping to prevent overheating. The heat transfer enhancement of the graphene coating is also anticipated for other shapes of fins, including parallel fins [26], triangular fins [27], rectangular fins [28], etc. Qualitatively, heat transfer enhancement is expected to depend on the coating thickness, regardless of the shape of the fin.

4. Conclusion

In this study, conjugate heat transfer numerical simulations were performed on graphene coated pin fin. The influences of air velocity, graphene coating thickness, and pin fin length were examined.

Numerical results show that the application of graphene as the coated material on pin fin is favourable for thermal dissipation application. The enhancement in heat transfer can be achieved, regardless of the air velocity and pin fin length. Thicker graphene coating is preferred as more heat can be transferred via conduction through the graphene coating. Examined on $5\ D$ long pin fin, applying graphene coating of one-tenth of the pin fin diameter, the temperature of the pin fin can be significantly reduced by 8.22 K. At the longest pin fin considered with $25\ D$ length, the thermal resistance can be reduced up to 56.60 % using $0.1\ D$ thick graphene coating. Based on the outcomes of this study, the implementation of this coating can be employed for high heat dissipation application utilizing longer pin fin.

Acknowledgement

This work was supported by the Universiti Sains Malaysia, Research University Team (RUTeam) Grant Scheme (Grant Number: 1001/PMEKANIK/8580012).

Nomenclature

A	Surface area [m^2]
c	Specific heat capacity [J kg^{-1}K^{-1}]
D	Diameter [m]
e	Relative error [%]
H	Pin fin height [m]
k	Thermal conductivity [W m^{-1}K^{-1}]
L	Length [m]
M	Mesh
P	Pin fin position [m]
p	Pressure [Pa]
q''	Heat flux [W m^{-2}]
R	Thermal resistance [K W^{-1}]
Re	Reynolds number
T	Temperature [K]
t	Thickness [m]
$\vec{V}$	Velocity [m s^{-1}]

Greek symbols

Δ	Difference
μ	Dynamic viscosity [kg m^{-1} s^{-1}]
ρ	Density [kg m^{-3}]

Subscripts

base	Pin fin base
con	Conventional pin fin
f	Fluid
max	Maximum
s	Solid
x	Axial
y	Vertical
z	Transverse

References

[1] Gan, J. S., Hung, Y. M., Remarkable thermal performance enhancement of micro heat pipes with graphene-nanoplatelet nano-wicks, *Nanomaterials*, *13* (2023), 2, 232

[2] Balandin, A. A., *et al.*, Superior thermal conductivity of single-layer graphene, *Nano Letters*, *8* (2008), 3, pp. 902-907

[3] Ghosh, S., Sharma, M., Electron optics with magnetic vector potential barriers in graphene, *Journal of Physics: Condensed Matter*, *21* (2009), 29, 292204

[4] Seol, J. H., *et al.*, Two-dimensional phonon transport in supported graphene, *Science*, *328* (2010), 5975, pp. 213-216

[5] Yu, Z., *et al.*, Highly thermal conductive epoxy composites enabled by 3D graphene/Cu-based dual networks for efficient thermal management, *Composites Communications*, *46* (2024), 101845

[6] Wu, R., *et al.*, Filling the gap: thermal properties and device applications of graphene, *Science China Information Sciences*, *64* (2021), pp. 1-17

[7] Amirpour, S., *et al.*, Highly thermal conductive graphene-based heatsink tailored for electric propulsion SiC-based inverter, *Applied Thermal Engineering*, *243* (2024), 122548

[8] Cheng, C., *et al.*, Evaluation of surfactants on graphene dispersion and thermal performance for heat dissipation coating, *Polymers*, *14* (2022), 5, 952

[9] Lv, L., *et al.*, Graphene-based thermal interface materials: an application-oriented perspective on architecture design, *Polymers*, *10* (2018), 11, 1201

[10] Hu, J., *et al.*, Significant enhancement of metal heat dissipation from mechanically exfoliated graphene nanosheets through thermal radiation effect, *AIP Advances*, *7*, (2017), 5

[11] Cheng, S., *et al.*, Co-enhancement of thermal conduction and radiation through morphologies controlling of graphene functional layer for chip thermal management, *Nano Research*, *17* (2024), 10, pp. 8885-8892

[12] Kung, F., Yang, M.-C., Improvement of the heat-dissipating performance of powder coating with graphene, *Polymers*, *12* (2020), 6, 1321

[13] Fang, J., *et al.*, Thermal management of a semiconductor laser array based on a graphite heat sink, *Applied Optics*, *58* (2019), 28, pp. 7708-7715

[14] Praveen, B., *et al.*, Heat transfer performance of graphene nano-platelets laden micro-encapsulated PCM with polymer shell for thermal energy storage based heat sink, *Applied Thermal Engineering*, *156* (2019), pp. 237-249

[15] Lv, S., *et al.*, The passive cooling and thermal properties of the dual functional film composed of graphene and PDMS-TiO2: application in the passive heat sink, *Solar Energy Materials and Solar Cells*, *276* (2024), 113077

[16] Dai, W., *et al.*, Ultralow interfacial thermal resistance of graphene thermal interface materials with surface metal liquefaction, *Nano-Micro Letters*, *15* (2022), 1, 9

[17] Chen, L., *et al.*, Effect of graphene coating on the heat transfer performance of a composite anti-/deicing component, *Coatings*, *7* (2017), 10, 158

[18] Wang, J.-X., *et al.*, Nano-enhanced graphite/phase change material/graphene composite for sustainable and efficient passive thermal management, *Advanced Science*, *11* (2024), 38, 2402190

[19] Teng, T.-P., *et al.*, Enhanced heat dissipation performance of automotive LED lamps using graphene coatings, *Polymers*, *14* (2022), 1, 50

[20] Pradhan, S. K., *et al.*, Graphene-incorporated aluminum with enhanced thermal and mechanical properties for solar heat collectors, *AIP Advances*, *10* (2020), 065016

[21] Choong, J.Y., *et al.*, Numerical assessment on heat transfer performance of double-layered oblique fins micro-channel heat sink with Al2O3 nanofluid, *Thermal Science*, *26* (2022), No. 1B pp. 477-488

[22] Soo, Y. H., *et al.*, Heat transfer enhancement of staggered water-droplet grooved microchannel heat sink using Al_2O_3 nanofluid, *Thermal Science*, *28* (2024), No. 3B pp. 2477-2490

[23] Shkarah, A. J., *et al.*, A 3D numerical study of heat transfer in a single-phase micro-channel heat sink using graphene, aluminum and silicon as substrates, *International Communications in Heat and Mass Transfer*, *48* (2013), pp. 108-115

[24] Mann, S., *et al.*, Thermodynamic properties of pure and doped (B, N) graphene, *RSC Advances*, *6* (2016), 15, pp. 12158-12168

[25] Ghajar, A. J.,Yunus, A., Cengel, D., *Heat and Mass Transfer: Fundamentals and Applications*. McGraw-Hill Education, 2014

[26] Abdelmohimen, M. A., *et al.*, Numerical investigation of using different arrangement of fin slides on the plate-fin heat sink performance, *Thermal Science*, *25* (2021), No. 6B, pp. 4683-4693

[27] Roy, R., Kundu, B., Effects of fin shapes on heat transfer in microchannel heat sinks, *Heat Transfer—Asian Research*, *47* (2018), 4, pp. 646-659

[28] Xie, G., *et al.*, Analysis of micro-channel heat sinks with rectangular-shaped flow obstructions, *Numerical Heat Transfer, Part A: Applications*, *69* (2016), 4, pp. 335-351

Received: 11.11.2024.

Revised: 15.02.2025.

Accepted: 30.04.2025.